LYSO-based Precision Timing Detectors with SiPM Readout

A. Bornheim[a], M. H. Hassanshahi[b], M. Griffioen[a], J. Mao[a], A. Mangu[a], C. Peña[a], M. Spiropulu[a], S. Xie[*,a], Z. Zhang[a]

[a] *California Institute of Technology, Pasadena, CA, USA*
[b] *Institute for Research in Fundamental Science, Tehran, Iran*

Abstract

Particle detectors based on scintillation light are particularly well suited for precision timing applications with resolutions of a few 10's of ps. The large primary signal and the initial rise time of the scintillation light result in very favorable signal-to-noise conditions with fast signals. In this paper we describe timing studies using a LYSO-based sampling calorimeter with wavelength-shifting capillary light extraction and silicon photomultipliers as photosensors. We study the contributions of various steps of the signal generation to the total time resolution, and demonstrate its feasibility as a radiation-hard technology for calorimeters at high intensity hadron colliders.

Key words: LYSO, Silicon Photomultiplier, Precision Timing, picosecond, scintillation, calorimeter

1. Introduction

Precise time of arrival measurements have recently drawn much attention in the context of detector R&D for the high luminosity upgrade of the Large Hadron Collider (HL-LHC) as well as for future high energy hadron colliders. These hadron colliders must provide large instantaneous luminosity well above 10^{35} cm^{-2}s^{-1}. With current accelerator and particle detector capabilities, such a high instantaneous luminosity will result in up to 200 simultaneous interactions (pileup) per bunch crossing. The ability to associate the origin of particles with different interaction points is crucial to the physics program, and precision timing would provide a new tool for achieving it, independently from track reconstruction.

Therefore, the crucial ability to identify the origin of the particles produced at the different interaction points will be severely degraded. Precision timing detectors can be used to recover the ability to discriminate between particles produced by different inelastic collisions [1]. For colliding particle beams with time spread of the order of 150–200 ps, as projected for the HL-LHC, a detector that can measure the time of arrival of particles can identify and reject particles from pileup collisions based on their time of arrival. Therefore with a timing detector with a timing precision of 20–30 ps, the

*Corresponding author
Email address: sixie@hep.caltech.edu (S. Xie)

number of pileup collisions which cannot be rejected based on their time of arrival will be about 20 to 40 and is similar to operational conditions in Run 2 of the LHC. A timing resolution in the range of $30 - 50$ ps is also very interesting for optical time projection chambers which are discussed for large volume detectors in neutrino experiments and neutrino-less double-beta decay [2, 3].

In our previous work in Ref. [4], we demonstrated the feasibility of achieving 30 ps resolution for electromagnetic showers using a sampling calorimeter based on LYSO crystal scintillators. Using micro-channel plate photomultipliers (MCP-PMTs) to read out photons on the edge of each LYSO layer, we achieved a time resolution of 55 ps for electrons with 32 GeV of energy. Using wavelength-shifting fibers to extract the light into the MCP-PMTs, we achieved a time resolution close to 100 ps. We concluded that the goal of 30 ps time resolution was within reach provided that we can realize similar performance using more economical photodetectors, extract the light using means that are radiation-hard, and achieve improved light collection efficiency. In this paper, we report on updated studies that demonstrate the time resolution performance using silicon photomultiplier (SiPM) detectors that are more economically scalable to the size of modern collider experiments, and radiation-hard wavelength-shifting quartz capillaries that can maintain its transparency under the harsh radiation conditions of the HL-LHC.

The paper is organized as follows. In Sec. 2 we give a brief overview of the SiPM sensors in the context of our research. In Sec. 3 we describe the experimental techniques we employ in our precision timing measurements as well as the specific setups we used for the studies presented in this paper. In Sec. 4.1 we present the results of timing measurements using SiPMs as photodetectors to read out scintillation light from LYSO crystals exposed to electrons in the GeV energy range. In Sec. 4.2 we evaluate the impact of the intrinsic timing performance of SiPM devices on the calorimeter time measurement by measuring the time resolution for SiPMs injected with light from a fast laser.

2. SiPM

SiPMs are pixelated photodetectors that are increasingly used in contemporary high-energy physics experiments. Their compactness and form factor make them ideal for many applications including calorimeters [5] and charged particle detectors. They are also widely used for positron emission tomography (PET) detectors together with LYSO scintillating crystals for medical imaging purposes [6], where new studies have improved the timing resolution below 100 ps [7] and can yield substantial improvements in spatial resolution and imaging capabilities. The size of each SiPM device typically ranges between 1×1 mm^2 and 6×6 mm^2, with the size of each pixel ranging between 10 μm to 50 μm. SiPMs operate at relatively high gain between 10^5 and 10^6, and have single photon detection efficiency ranging from 10% to 50%.

SiPMs have a typical thermal dark count rate of about 0.1 MHz/mm^2 at room temperature, which can be strongly decreased when operated at lower temperatures. Typical operational temperatures range from 20°C to 30°C, but can be as low as −30°C. SiPMs have been tested for the impact of radiation damage up to an equivalent neutron rate of 2×10^{14} cm^2, and its performance have been shown to be robust when operated at temperatures below 5°C [8, 9]. However, when operated at the same temperature, the thermal dark count rate increases significantly with large irradiation. The SiPMs used for our studies are Hamamatsu MPPC S12571-010P and S12571-015P both of size

1×1 mm^2, and S12572-15C and S12572-25C both of size 3×3 mm^2. These SiPMs are chosen to allow us to study the impact of the size of the sensitive area and the size of individual pixels on the timing performance. Studies of the impact of SiPMs from alternative manufacturers are left for future work. Some relevant details of the SiPM parameters are summarized in Table 1 below.

Table 1: Summary of performance parameters for SiPMs used in our studies.

Parameter	S12571-010C	S12571-015C	S12572-15C	S12572-25C
Photosensitive area	1×1mm^2	1×1mm^2	3×3mm^2	3×3mm^2
Pixel Pitch	10μm	15μm	15μm	25μm
Number of Pixels	10000	4489	40000	14400
Dark Count Rate	0.1 MHz	0.1 MHz	1 MHz	1 MHz
Gain	1.35×10^5	2.3×10^5	2.3×10^5	5.15×10^5
Terminal Capacitance	35 pF	35 pF	320 pF	320 pF
Spectral Response Range	320-900 nm	320-900 nm	320-900 nm	320-900 nm
Peak Sensitivity Wavelength	470 nm	460 nm	460 nm	450 nm

3. Setup and Experimental Apparatus

We performed measurements of SiPM properties in the laboratory using signals from a class 3R PiLas laser which produces light at a wavelength of 407 nm. Beam measurements were performed at the H4 beam-line of the CERN North-Area test-beam facility, which provides secondary beams of energies ranging between 20 GeV and 400 GeV. Electrons can be provided from tertiary beams up to 250 GeV with acceptable efficiency. The beams are composed of a mixture of electrons and pions. The electron fraction in the beam is typically larger than 75% and close to 100% for beam energy above 100 GeV.

The data acquisition (DAQ) system uses a CAEN V1742 switched capacitor digitizer based on the DRS4 chip [10], whose electronic time resolution has been measured to be 4 ps. Data readout for the laser-based measurements are triggered by an external digital trigger signal, while at the H4 beamline readout is triggered by a signal in a photomultiplier tube coupled to a 3 cm $\times$ 3 cm plastic scintillator located about one meter upstream from our detectors. A micro-channel plate photo-multiplier (MCP-PMT) detector is used to provide a very precise reference time-stamp in order to measure the time resolution of the SiPM signals.

3.1. Setup for Laser-based SiPM Timing Measurements

SiPMs are mounted on a printed circuit board (PCB) with the circuit shown in Figure 1. The high-pass filter is used to decrease the rise-time of signal pulses by removing low-frequency components of the signal pulse. As a consequence, the resulting signal pulse will be smaller in amplitude and will have a faster rise-time. The SiPMs are mechanically attached to an optical breadboard enclosed within a box lined with copper foil for RF shielding. The laser is injected via a light guide fiber mounted on an optical holder. The laser beam is immediately split by a 50/50 beam splitter and half of the light is directed

onto the MCP-PMT while the other half of the light is directed onto the SiPM under test. A photograph of the setup is shown in Figure 2. The Photek-240 MCP-PMT is used as the reference time detector whose time resolution has been measured to be below 7 ps for beam particles [11]. To cover a large range of laser beam intensity, neutral density (ND) filters with ND number between 0.2 and 2.4 are placed between the beam splitter and the SiPM under test.

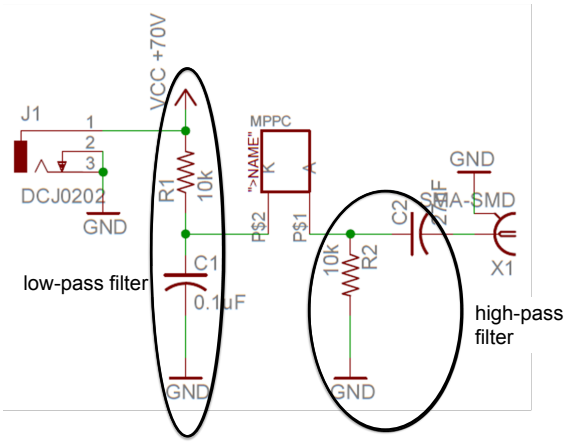

Figure 1: A schematic diagram of the circuit used to read out the SiPMs.

3.2. Setup for Timing Measurements of Scintilators with SiPM readout.

The experimental setup we use for the calorimetric timing measurements is shown diagrammatically in Fig. 3 and consists of a single cell of a sampling calorimeter with 29 alternating layers of LYSO crystal and tungsten absorber, known as a Shashlik sampling calorimeter configuration. The lateral dimensions are 14×14 mm^2. The total depth of the cell is about 11.5 cm with the LYSO layers having a thickness of 1.5 mm. The same cell has been used to measure the timing performance in comparison to the timing performance of a single monolithic crystal of LYSO [4]. A scintillator counter of size 1×1 cm^2, mounted close to the calorimeter cell, is used to select events impinging on the center of the calorimeter cell. The scintillation light from the LYSO plates is extracted with four wavelength-shifting (WLS) fibers with 1 mm diameter. The fibers are coupled to four different types of Hamamatsu SiPMs with 10, 15 and 25 μm pixel size and 1×1 mm^2 and 3×3 mm^2 sensor size [12]. SiPMs are mounted on a printed circuit board (PCB) with the circuit shown in Figure 1. The high-pass filter is used to decrease the rise-time of signal pulses by removing low-frequency components of the signal pulse. As a consequence, the resulting signal pulse will be smaller in amplitude and will have a faster rise-time. We do not amplify the output signal of the SiPMs, only exploiting the very large light yield of the LYSO scintillator and the intrinsic amplification of the SiPMs. All four SiPMs were operated at a bias voltage of 70 V, and due to the variance of breakdown voltages of the different SiPMs the operational gain was different for each channel. A labeled photograph of the setup in the H4 beamline is shown in Figure 4.

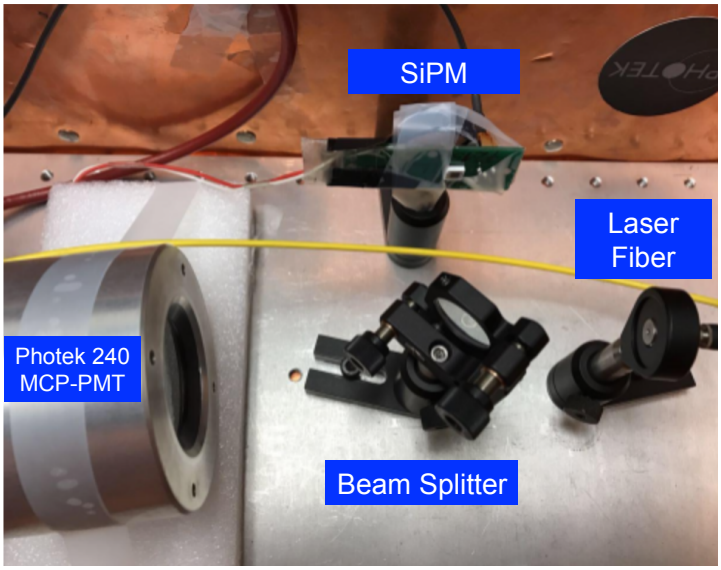

Figure 2: Photograph of the Laser-based SiPM timing measurement setup.

More details of the calorimetric performance of the Shashlik configuration are discussed in references [13] and [14].

In addition to plastic WLS fibers we also tested quartz capillaries filled with liquid wavelength shifter using DSB as a wavelength-shifting agent [15]. To optically couple the quartz capillaries to the SiPMs we use a clear plastic fiber light guide which is connected to the end of the quartz capillary with a metal sleeve tube. The same clear fiber coupler is used for the plastic WLS fibers to maintain equivalent light collection efficiency. The ratio of the light collection efficiency between the plastic fibers and the quartz capillaries approximately scales with the ratio of the diameter of the plastic fiber and the liquid core of the quartz capillary. This ratio is about 3 for the fibers and capillaries we used.

The Photek 240 MCP-PMT, used as the reference time detector, is placed behind the calorimeter cell and detects secondary shower particles escaping from the Shashlik calorimeter cell as we did in our previous studies [4]. The time resolution is extracted by measuring the time difference between the reference counter and the calorimeter cell over an ensemble of shower events. The time stamp for the reference counter and calorimeter cell is extracted from a Gaussian fit to the peak and a linear fit to the rising edge, respectively, as described below in Section 3.3.

We measure the timing performance of the calorimeter cell with high energy beams in a range between 20 GeV and 200 GeV. Selection cuts on the signal amplitude in the Shashlik cell suppresses the pion contamination in the beam. The impact point of the electrons onto the calorimeter cell is measured with a fiber hodoscope with a precision of better than 1 mm. As timing measurements are affected by shower containment, we restrict the time measurements to events where shower containment is large. This is achieved by using events where the beam particle impacts in the center of the calorimeter cell within a restricted area between 2×2 mm^2 and 6×8 mm^2 depending on the exact

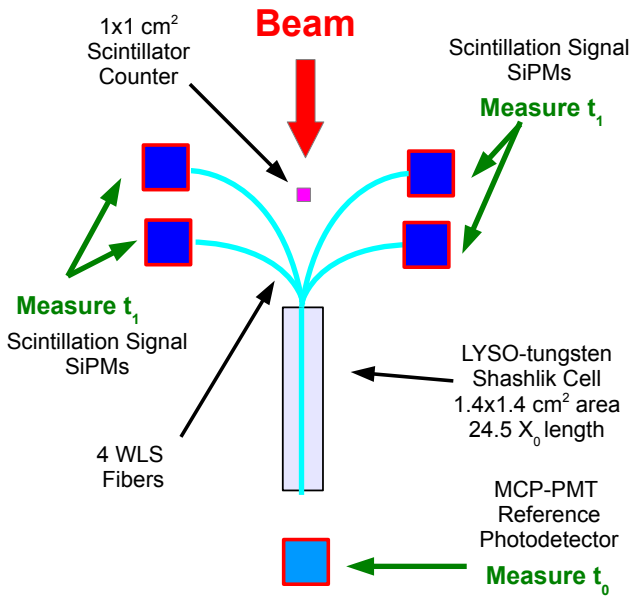

Figure 3: Schematic diagram of the testbeam experimental setup.

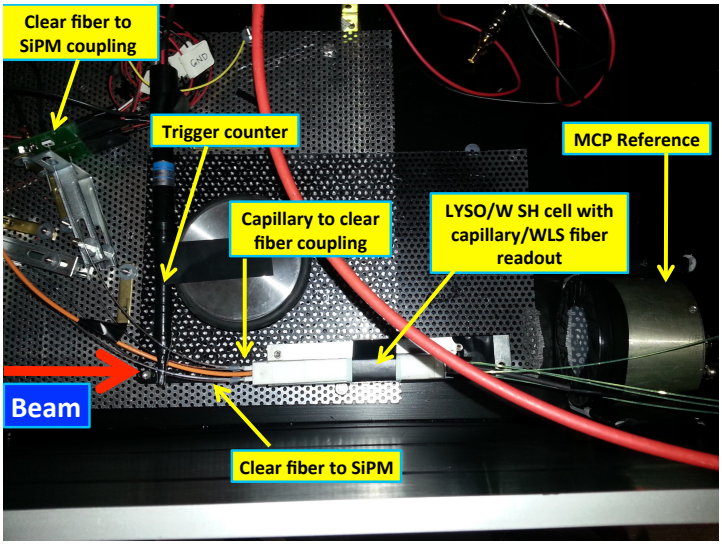

Figure 4: Photograph of the timing measurement setup in the H4 beamline.

setup.

3.3. Timestamp Reconstruction

The time-stamp for all signals is reconstructed by fitting the pulse waveform with an appropriate functional form. Signal pulses from the MCP-PMTs as well as direct laser light signals on the SiPMs exhibit a very fast rise and decay. Therefore, we fit a Gaussian function to a 1.4 ns window around the peak of the pulse and extract the time-stamp as the mean parameter of the Gaussian function. Scintillation signal pulses read out by the SiPM sensors have a much longer decay time. For these signals, we fit a linear function to time sample points between 10% and 60% of the pulse maximum and the time-stamp is assigned as the time at which the fitted linear function rises to 20% of the pulse maximum. More details of the time-stamp reconstruction can be found in reference [4].

4. Timing Measurements

While SiPMs feature a rise time around 1 ns, slower than the rise time of MCPs, they allow a very good timing performance for large, coherent signals. We present measurements of the timing performance for a LYSO-based sampling calorimeter read out by wavelength-shifting light fibers connected to SiPMs. We also discuss the impact of the intrinsic timing performance of SiPMs on the calorimeter timing by performing measurements using a picosecond laser shining directly onto the SiPMs.

4.1. Timing Performance Results from Calorimeter with SiPM Readout

Four different SiPMs are used to read out the four light fibers. As the SiPMs and fibers each have different gain and light collection efficiency, the signal amplitudes vary for the four different channels. In Figure 5 we show the time resolution of the four individual fibers as a function of their respective signal amplitudes for both the DSB-doped fibers and the DSB-filled quartz capillaries. Each data point corresponds to the mean measured signal amplitude and time resolution from a dataset with different beam energy. We observe that the time resolution improves as the beam energy and signal amplitude increases. The best time resolution per fiber is around 60 ps for all of the channels, but the amplitude at which this performance is achieved varies. Another important observation is that the time resolution measured from the WLS fibers fall on the same curve as the time resolution measured from the quartz capillaries. We conclude that the method of light extraction impacts the time resolution only through its effect on the signal amplitude, and no additional time jitter is introduced.

As the time measurement precision depends on the rise time of the pulse we also measure the time resolution as a function of the rise time for signals observed in the calorimeter cell shown in Figure 6. Each data point corresponds to a measurement of mean rise time for datasets taken using different beam energy. The capacitance of the high-pass filter for the 3×3 mm^2 SiPM with 25 μm pixel size is significantly larger than the capacitance for the other three SiPMs, resulting in signals with larger amplitude but also larger rise time.

In our previous study [4] that used MCPs as photodetectors, the rise time was measured to be about 3.0 ns and did not have any dependence on the signal amplitude. The

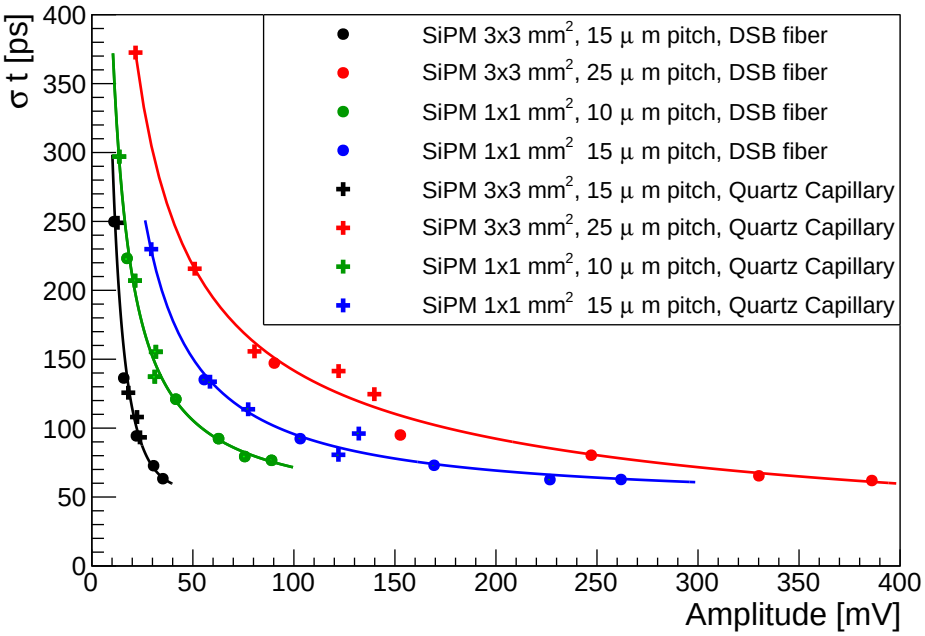

Figure 5: The measured time resolution is shown as a function of the signal amplitude for each individual read-out fiber and SiPM. The data for each SiPM consists of two sets, one with the DSB-doped WLS plastic fiber shown as dots and one with the capillaries filled with a liquid DSB-based WLS shown as squares.

very fast rise time of less than 150 ps of the MCP and its signal amplitude linearity implied that the rise time was dominated by the time constant of the wavelength shifter. In contrast, for the data presented here using SiPMs as photodetectors, we observe that the rise time varies between 1.4 ns and 6 ns. We attribute this effect to the fact that there are so many scintillation photons reaching the SiPM that the signal is in the non-linear saturation regime of the SiPM. As a result the signal appears to reach its maximum faster. This effect is reproduced by a simple simulation where we take a scintillation light pulse with a rise time of 3 ns impinging upon a 1×1 mm^2 SiPM with 10 μm pixel size and simulate a dead time of 5 ns for each pixel. The resulting rise time as a function of light input is shown in Figure 7, and shows a decreasing rise time as the amount of light increases.

We show the time resolution measured as a function of the beam energy for signals read out by DSB-doped WLS fibers and quartz capillaries in Figure 8. Finally, by combining the measured timestamp from all four SiPM channels, we can significantly improve the time resolution. The combined time resolution measurements for the DSB WLS fibers and the quartz capillaries are shown in Fig 9 and demonstrate that we can achieve time resolution of 42 ps for high energy electromagnetic showers. The timing performance we achieve with the SiPM readout is slightly better than the performance achieved with an MCP-PMT as in our previous publication [4], where we achieved 90,

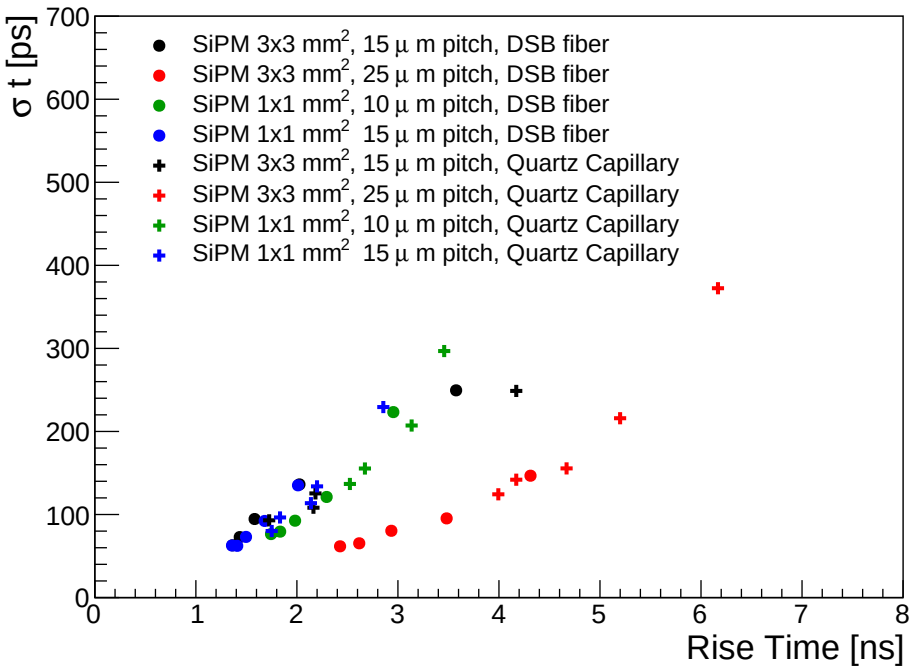

Figure 6: Time resolution is measured as a function of the rise time for the four different SiPMs. The data recorded with the DSB WLS fibers and the quartz capillaries are distinguished as dots and squares, respectively.

70, and 60 ps at 50, 100, and 150 GeV respectively.

The light extraction efficiency of capillaries with liquid WLS remains sufficiently high for dose rates of 100 Mrad and beyond and for fluences of 10^{14} protons/cm^2 and beyond [14]. This result demonstrates the feasibility of achieving good time resolution using a sampling calorimeter based on LYSO, which can survive in dense hadronic collision environments. The timing performance could be further improved by increasing the signal size, for example by using larger diameter capillaries or increasing the calorimeter sampling fraction.

4.2. Timing Performance Results for Laser Pulses

To evaluate the impact of the intrinsic timing performance of the SiPMs on the time resolution measured for the sampling calorimeter signals, we performed laser-based measurements for two types of SiPMs: a Hamamatsu S12571-015P Multi-Pixel Photon Counter (MPPC) with an area of 1×1 mm^2 and pixel pitch size of 15 μm, and a Hamamatsu S12572-25C MPPC with an area of 3×3 mm^2 and pixel pitch size of 25 μm. These two devices capture the impact on the timing performance due to differences in the pixel pitch size and the total area. Examples of the digitized waveforms for signals from both SiPMs are shown in Figure 10.

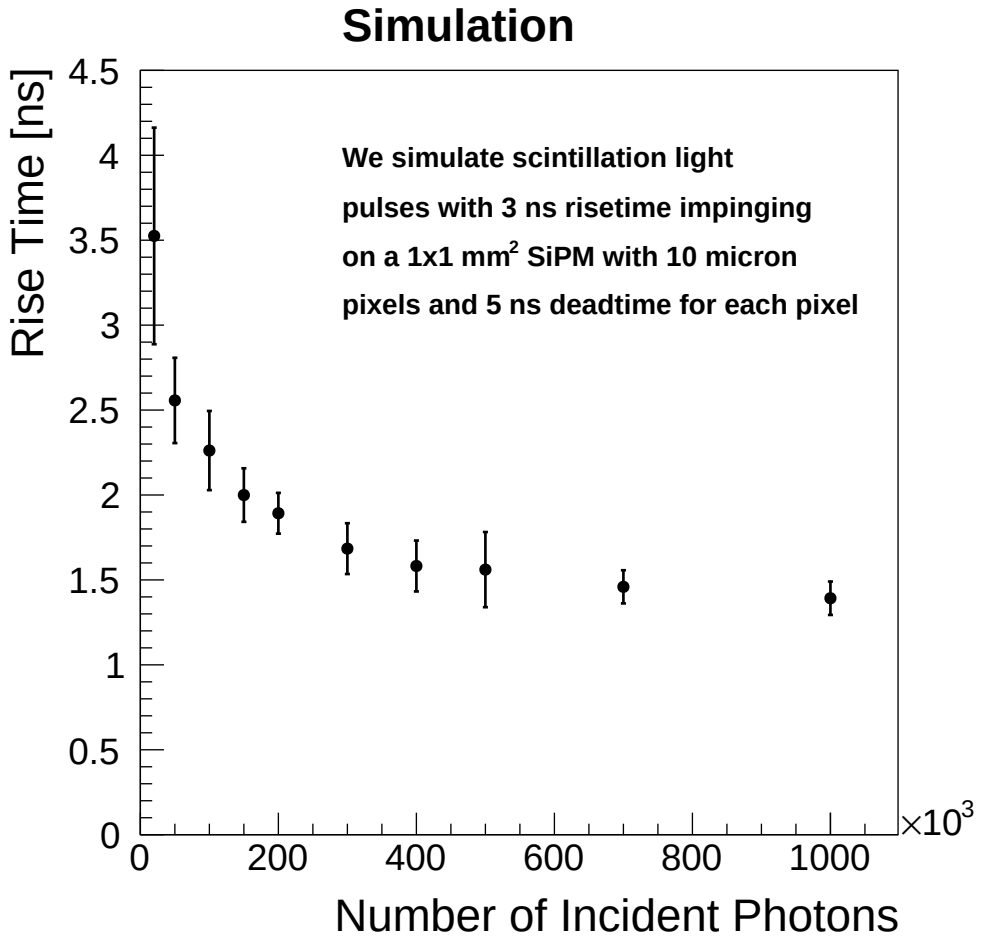

Figure 7: We simulate a scintillation light pulse with a rise time of 3 ns impinging upon a 1×1 mm^2 SiPM with 10 μm pixel size where each pixel has a dead time of 5 ns. The resulting rise time of the full signal pulse is plotted as a function of the amount of input scintillation light.

Using several different ND filters we controlled the intensity of the photon beam impinging upon the SiPMs under test and achieved a large dynamic range of input light intensity ranging from a single incident photon to a few hundred. In Figure 11, we show the integrated charge distribution for two example scenarios from which we can clearly distinguish different peaks corresponding to different number of photoelectrons detected by the SiPMs.

Using this setup, we measure the timestamps reconstructed from the SiPM signals with respect to the reference MCP-PMT timestamp over an ensemble of events triggered by the external laser trigger. The sigma parameter of a gaussian fit to this distribution is taken as the time resolution measurement. As the number of photoelectrons detected can be clearly distinguished based on the amplitude or charge collected, we can study the

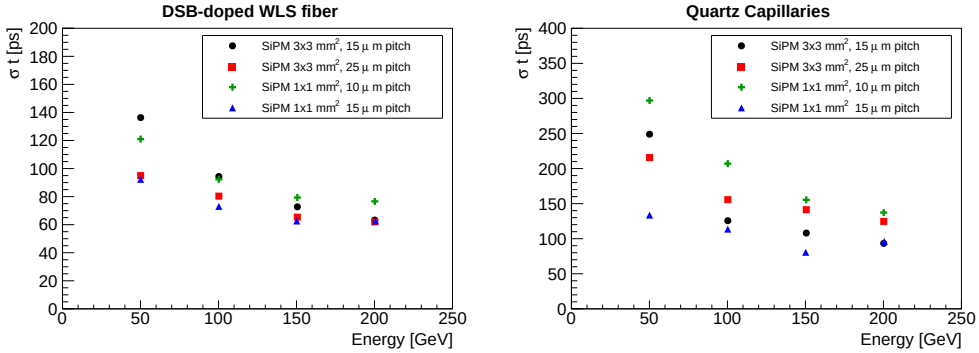

Figure 8: Time resolution measured in the sampling calorimeter cell using the signal of each of the SiPMs individually as a function of the beam energy. The data taken using DSB-doped WLS fibers are shown on the left and the data taken using DSB-filled quartz capillaries are shown on the right

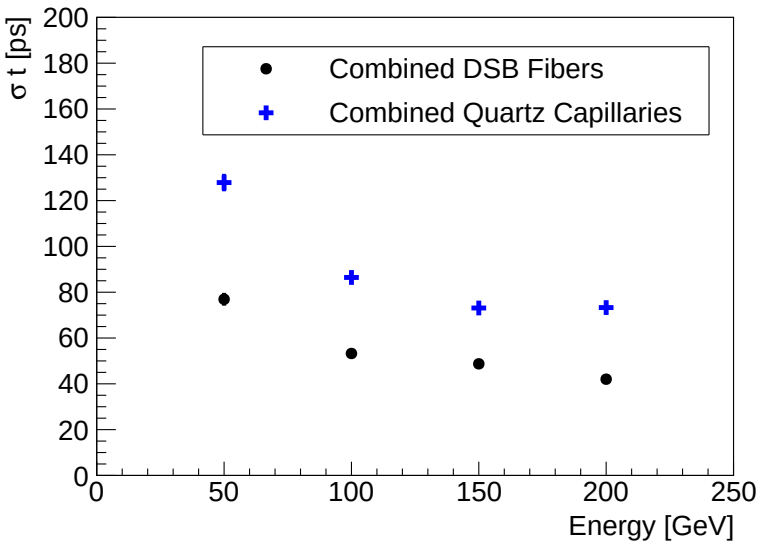

Figure 9: Time resolution measured in the sampling calorimeter cell combining signals from all four SiPMs is shown as a function of the beam energy. The data recorded with the DSB-doped WLS fibers and the DSB-filled quartz capillaries are distinguished as dots and squares.

dependence of the time resolution on the number of photoelectrons. These measurements are shown in Figure 12. The amplitude for a single photoelectron signal is estimated to be 0.6 mV for the 1×1 mm^2 S12571-015P SiPM and 0.1 mV for the 3×3 mm^2 S12572-25C SiPM. The data points are fitted to a functional form that includes a $1/N$ term to model the electronic noise, and a $1/\sqrt{N}$ stochastic term. Using these measurements, we can compare the time resolution of laser light signals on SiPMs from Figure 12 to the time resolution of electromagnetic shower signals from the WLS fiber in Figure 5

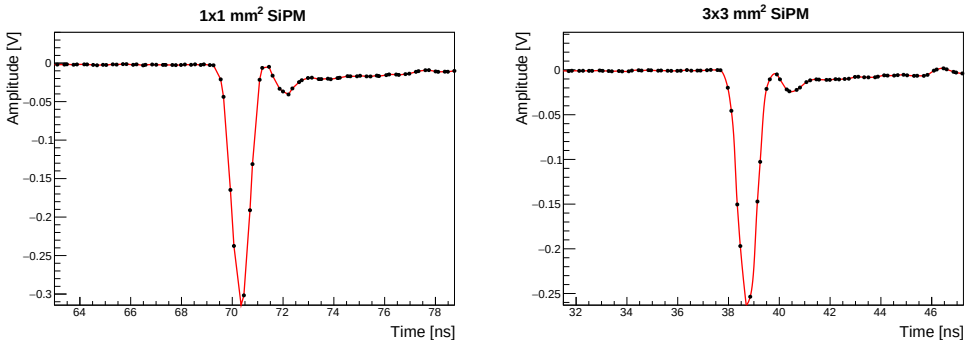

Figure 10: Digitized waveforms of the signals from the PiLas laser in the S12571-015P (left) and S12572-25C (right) SiPMs.

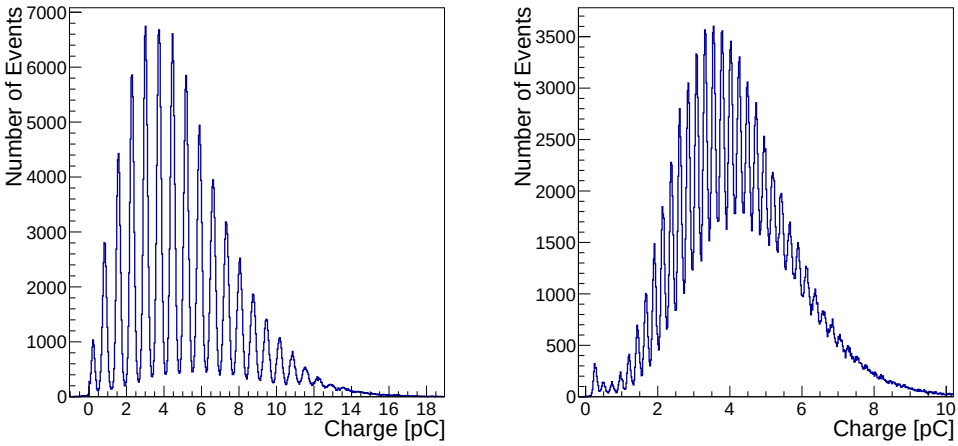

Figure 11: The distribution of integrated charge from the S12571-015P SiPM sensor for data taken with an ND filter of 1.8 (left), and an ND filter of 1.4 (right). A 10 db attenuator has been used for the plot on the right. The peaks corresponding to different discrete numbers of photoelectrons detected by the SiPM is clearly evident.

and conclude that the intrinsic timing performance of SiPM devices have very limited impact on the calorimeter time resolution. Instead, the time resolution of the calorimeter is dominated by the impact of the wavelength shifter and the corresponding increased rise time. An additional contribution to the timing resolution of the calorimeter cell may arise from longitudinal shower fluctuations. Shower depth fluctuations result in fluctuations in the time it takes for the shower to propagate into the calorimeter cell as well as for the scintillation light to propagate out of the cell thought the light guides. This contribution to the time resolution is evident only if the signal is extracted at the front of the calorimeter cell because a fluctuation in the shower depth will not be compensated by a corresponding change in the optical signal transport path length. Such effects have been observed in timing studies for the CMS ECAL [16].

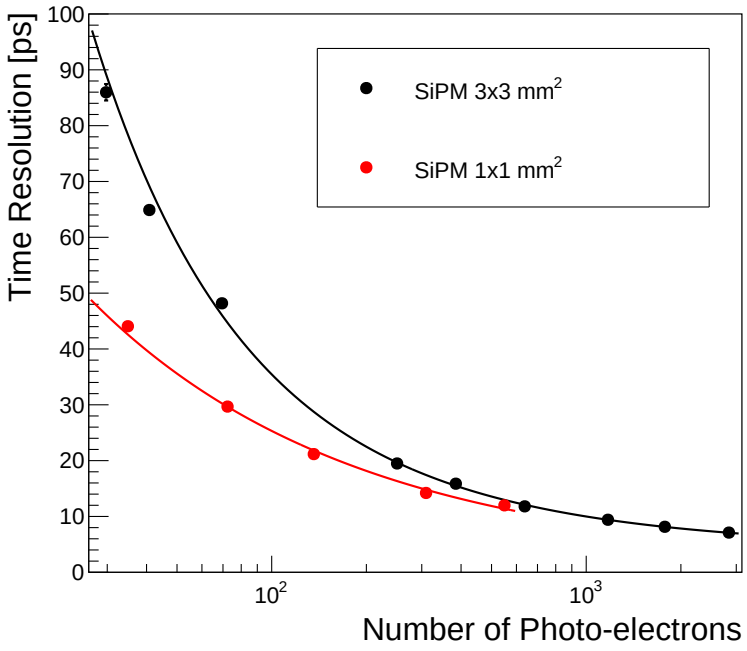

Figure 12: The time resolution is measured as a function of the number of photo-electrons detected by the SiPMs under test. The black points show measurements using the 3×3 mm^2 SiPM, and the red points show measurements using the 1×1 mm^2 SiPM. The data points are fitted to a functional form that includes a $1/N$ term to model the electronic noise, and a $1/\sqrt{N}$ stochastic term.

Finally, by removing all ND filters and increasing the laser output intensity to near maximum, we can measure the time resolution for a very large number of photons to probe for the ultimate time resolution that one could achieve with a near infinitely large signal. In Figure 13 we show the SiPM time distributions for such a scenario, and observe that the resolution is 12 ps for the 1×1 mm^2 S12571-015P SiPM and 7 ps for the 3×3 mm^2 S12572-25C SiPM. The latter measurement is also impacted by the limitation of the digitizer electronics as its time resolution is 4 ps.

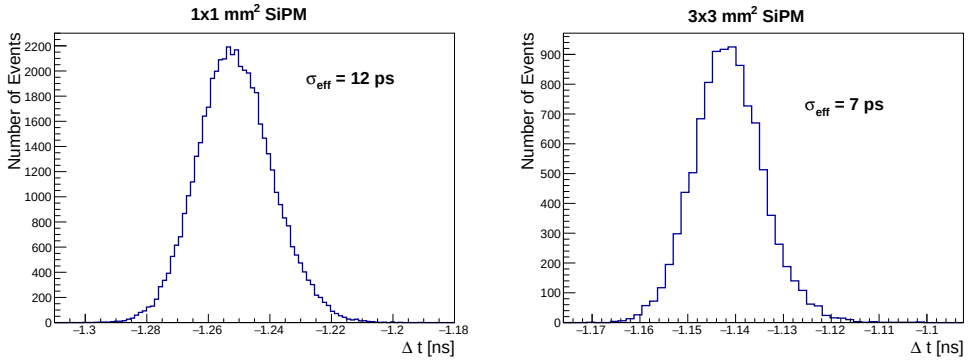

Figure 13: The SiPM time distribution and resolution measured for laser signals at high laser intensity. The resolution is characterized by σ_{eff}, which is the width obtained by integrating outwards from the peak to achieve 68% coverage.

5. Discussion and Summary

In our previous study [4], we achieved a time resolution of 110 ps for 32 GeV electromagnetic showers using DSB-doped WLS fibers for light readout at both ends of the fiber. The two main goals achieved in the present study are to confirm similar or slightly improved timing performance using photodetectors that are economically scalable to collider experiment size and WLS fibers that can maintain its transparency under the harsh radiation conditions of the HL-LHC. Using commercially available SiPMs that are economically scalable, we achieved a time resolution of 75 ps (40 ps) for 50 GeV (200 GeV) electromagnetic showers using DSB-doped WLS fibers read out only at a single end of the fiber. This represents a 15% improvement over the previous result, with the possibility for additional improvement if light is read out from both ends of the WLS fibers.

Using quartz capillaries filled with a DSB-based liquid wavelength-shifting agent, specially designed to survive the high radiation environment of the HL-LHC, we achieved a time resolution of 130 ps (75 ps) for 50 GeV (200 GeV) electromagnetic showers. The difference in timing resolution with respect to the DBS-doped WLS fibers is solely due to degraded signal-to-noise ratio as the light collection efficiency is worse for the quartz capillaries. This result demonstrates feasibility towards a radiation-hard solution for the future. As the time resolution performance is driven primarily by the signal-to-noise ratio, SiPMs with larger gain, larger quantum efficiency, and higher light collection efficiency are preferred. Of those we tested, the SiPMs with larger pixel sizes achieved better time resolution as their gain are larger and they have better light collection efficiency due to reduced amount of insensitive area in between pixels. Based on these results, we are optimistic that further work on improving the optical coupling, improving the light collection efficiency of the quartz capillaries by optimizing the dimensions and the composition of the liquid WLS agent, and improving the noise properties of the SiPMs can yield further improved timing performance.

We have presented test-beam measurements of the timing performance of a LYSO-based sampling calorimeter read out via four wavelength-shifting fibers optically coupled to silicon photomultipliers (SiPMs). Time resolutions at the level of 60 ps is achieved for beam energies above 100 GeV for individual fibers and SiPMs. Combining all four

fibers yield time resolution measurements of about 42 ps. Using laser light injected directly onto SiPMs, we have demonstrated that the impact of the intrinsic time resolution of the SiPM devices is small and that the calorimeter time resolution is dominated by the impact of the wavelength shifter. Finally, we have shown that the use of quartz capillaries do not degrade the time resolution beyond the impact from a reduced signal amplitude. Therefore it is feasible that this radiation-hard solution using quartz capillaries can achieve the desired 30 ps time resolution performance if additional improvements in light collection efficiency can be achieved.

6. Acknowledgements

Supported by funding from California Institute of Technology High Energy Physics under Contract DE-SC0011925 with the United States Department of Energy. We thank the CERN test-beam facilities personnel for excellent beam conditions during our test-beam time. We also thank Paolo Meridiani and Francesco Micheli for their kind assistance on the setup of the DAQ system at the test-beam. We greatly appreciate the collaboration with Randy Ruchti who provided us with wavelength-shifting fibers doped with DSB as well as quartz capillaries filled with liquid DSB wavelength shifter.

References

[1] A. Bornheim, "On the Usage of Precision Timing Detectors in High Rate and High Pileup Environments," *PoS(Vertex2016)044*, 2016.

[2] C. Aberle, A. Elagin, H. J. Frisch, M. Wetstein, and L. Winslow, "Measuring Directionality in Double-Beta Decay and Neutrino Interactions with Kiloton-Scale Scintillation Detectors," *JINST*, vol. 9, p. P06012, 2014.

[3] E. Oberla and H. J. Frisch, "The design and performance of a prototype water Cherenkov optical time-projection chamber," *Nucl. Instrum. Meth.*, vol. A814, pp. 19–32, 2016.

[4] D. Anderson, A. Apresyan, A. Bornheim, J. Duarte, C. Pena, A. Ronzhin, M. Spiropulu, J. Trevor, and S. Xie, "On Timing Properties of LYSO-Based Calorimeters," *Nucl. Instrum. Meth. A*, vol. 794, pp. 7–14, 2015.

[5] V. Andreev *et al.*, "A high granularity scintillator hadronic-calorimeter with SiPM readout for a linear collider detector," *Nucl. Instrum. Meth.*, vol. A540, pp. 368–380, 2005.

[6] S. Vandenberghe, E. Mikhaylova, E. D'Hoe, P. Mollet, and J. S. Karp, "Recent developments in time-of-flight pet," *EJNMMI Physics*, vol. 3, p. 3, Feb 2016.

[7] S. Gundacker, E. Auffray, K. Pauwels, and P. Lecoq, "Measurement of intrinsic rise times for various L(Y)SO and LuAG scintillators with a general study of prompt photons to achieve 10 ps in TOF-PET," *Physics in Medicine & Biology*, vol. 61, no. 7, p. 2802, 2016.

[8] A. Heering *et al.*, "Effects of very high radiation on SiPMs," *Nucl. Instrum. Meth.*, vol. A824, pp. 111–114, 2016.

[9] Y. Musienko *et al.*, "Radiation damage studies of silicon photomultipliers for the CMS HCAL phase I upgrade," *Nucl. Instrum. Meth.*, vol. A787, pp. 319–322, 2015.

[10] S. Ritt, R. Dinapoli, and U. Hartmann, "Application of the DRS chip for fast waveform digitizing," *NIM* **A** *623 (2010) 486-488.*

[11] A. Ronzhin, S. Los, E. Ramberg, A. Apresyan, S. Xie, M. Spiropulu, and H. Kim, "Study of the timing performance of micro channel plate photomultiplier for use as an active layer in shower maximum detector," *Nucl. Instrum. Meth.*, vol. 795, pp. 288–292, 2015.

[12] `http://www.hamamatsu.com/resources/pdf/ssd/mppc_kapd0004e.pdf`.

[13] H. Li, "Longevity of the CMS ECAL and Scintillator-Based Options for Electromagnetic Calorimetry at HL-LHC," *IEEE Trans. Nucl. Sci.*, vol. 63, no. 2, pp. 580–585, 2016.

[14] L. Zhang, R. Mao, F. Yang, and R. Y. Zhu, "LSO/LYSO Crystals for Calorimeters in Future HEP Experiments," *IEEE Trans. Nucl. Sci.*, vol. 61, pp. 483–488, Feb 2014.

[15] B. Baumbaugh *et al.*, "Studies of wavelength-shifting liquid filled quartz capillaries for use in a proposed CMS calorimeter," in *Proceedings, 2015 IEEE Nuclear Science Symposium and Medical Imaging Conference (NSS/MIC 2015): San Diego, California, United States*, p. 7581951, 2016.

[16] Simone Pigazzini for CMS Collaboration, "Precision timing with PbWO crystals and prospects for a precision timing upgrade of the CMS electromagnetic calorimeter at HL-LHC." CALOR 2016, 2016.